INSTITUTE OF PHYSICS PUBLISHING SMART MATERIALS AND STRUCTURES
Smart Mater. Struct. **13** (2004) 153–160 PII: S0964-1726(04)71818-2

Wavelet-based active sensing for delamination detection in composite structures

Hoon Sohn, Gyuhae Park, Jeannette R Wait, Nathan P Limback and Charles R Farrar

Engineering Sciences and Applications Division, M/S T006, Los Alamos National Laboratory, Los Alamos, NM 87545, USA

Received 28 August 2003, in final form 6 November 2003
Published 15 December 2003
Online at stacks.iop.org/SMS/13/153 (DOI: 10.1088/0964-1726/13/1/017)

Abstract
In this paper a signal processing technique is developed to detect delamination on composite structures. In particular, a wavelet-based signal processing technique is developed and combined with an active sensing system to produce a near-real-time, online monitoring system for composite structures. A layer of piezoelectric patches is used to generate an input signal with a specific wavelet waveform and to measure response signals. Then, the response signals are processed by a wavelet transform to extract damage-sensitive features from the original signals. The applicability of the proposed method to delamination identification has been demonstrated by experimental studies of a composite plate under varying temperature and boundary conditions.

(Some figures in this article are in colour only in the electronic version)

1. Introduction

Since the 1960s, the ultrasonic research community has studied Lamb waves for the nondestructive evaluation of plates [1]. Lamb waves are mechanical waves with wavelengths of the same order of magnitude as the thickness of the plate. Because the Lamb waves travel long distances and can be applied with conformable piezoelectric (PZT) actuators/sensors that require little power, they may prove suitable for online structural health monitoring. In particular, the recent development of wavelet analysis has allowed the application of Lamb wave techniques to composite structures to flourish [2–7]. The advances in sensor and hardware technologies for the efficient generation and detection of Lamb waves and the increased usage of solid composites in load-carrying structures, particularly in the aircraft industries, has led to an explosion of studies that use Lamb waves for detecting defects in composite structures. However, much work needs to be accomplished in the area of manufacturing process control and nondestructive evaluation technologies.

This study contributes to the damage detection of composite structures by developing an improved wavelet-based signal processing technique that enhances the visibility and interpretation of the Lamb wave signals related to defects in a composite plate. In addition, a statistically rigorous damage classifier is developed to identify wave propagation paths affected by damage. Finally, a new damage location algorithm is proposed to locate damage based on signal attenuation rather than time-of-arrival information.

2. Test set-up

The overall test configuration of this study is shown in figure 1(a). The test set-up consists of a composite plate with a surface-mounted sensor layer, a personal computer with a built-in data acquisition system and an external signal amplifier. The dimensions of the composite plates are 60.96 cm × 60.96 cm × 0.6350 cm (24 in × 24 in × 1/4 in). The lay-up of this quasi-isotropic plate contains 48 plies stacked according to the sequence [6(0/45/-45/90)]s, consisting of Toray T300 graphite fibers and a 934 Epoxy matrix.

A commercially available thin film with embedded piezoelectric (PZT) sensors is mounted on one surface of the composite plate as shown in figure 1(b) [8]. A total of 16 PZT patches are used as both sensors and actuators to form an ‘active’ local sensing system. Because the PZTs produce

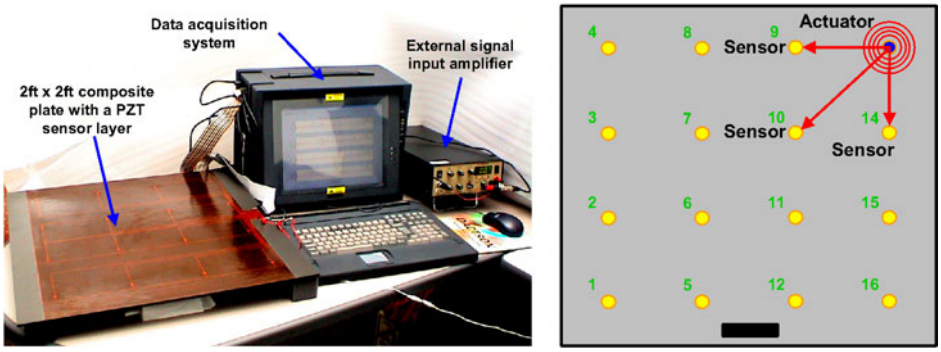

(a) Testing configuration (b) Layout of the PZT sensors/actuators

Figure 1. An active sensing system for detecting delamination on a composite plate.

an electrical charge when deformed, the PZT patches can be used as dynamic strain gauges. Conversely, the same PZT patches can also be used as actuators, because elastic waves are produced when an electrical field is applied to the patches. In this study, one PZT patch is designated as an actuator, exerting a predefined waveform into the structure. Then, the adjacent PZTs become strain sensors and measure the response signals. This actuator–sensor sensing scheme is graphically shown in figure 1(b). This process of Lamb wave propagation is repeated for different combinations of actuator–sensor pairs. A total of 66 different path combinations are investigated in this study. The data acquisition and damage identification are fully automated and completed in approximately 1.5 min for a full scan of the plate used in this study. These PZT sensor/actuators are inexpensive, generally require low power and are relatively non-intrusive.

The personal computer shown in figure 1(a) has built-in analog-to-digital and digital-to-analog converters, controlling the input signals to the PZTs and recording the measured response signals. Increasing the amplitude of the input signal yields a clearer signal, enhancing the signal-to-noise ratio. On the other hand, the input voltage should be minimized for field applications, requiring as little power as possible. In this experiment the optimal input voltage was designed to be near 45 V, producing 1–5 V output voltage at the sensing PZTs. PZTs in a circular shape are used with a diameter of only 0.64 cm (1/4 in). The sensing spacing is set to 15.24 cm (6 in). A discussion on the selection of design parameters, such as the dimensions of the PZT patches, sensor spacing and driving frequency, can be found in [2]. The data analysis and signal processing portion of this study is described in the following sections.

3. Lamb wave based damage detection

One of the unique aspects of this study lies in that a carefully designed input waveform is exerted into a structure to make the response signal more sensitive to damage. The use of a known and repeatable input makes the subsequent signal processing for damage detection much easier and repeatable. A similar approach to noise elimination in ultrasonic signals for flaw detection can be found in [9]. In addition, a multiresolution processing scheme based on wavelet analysis is developed to extract a portion of the response signal that is more amenable to signal interpretation for detecting defects. Finally, the vibration characteristics of the response signals are investigated under varying temperature and boundary conditions.

Since Lamb waves were initially studied for seismology applications in 1917 [10], damage detection techniques based on Lamb wave propagation have been investigated by many researchers over the last four decades because Lamb waves can propagate over long distances and cover relatively large areas of thin plates. Because the Lamb waves are typically dispersive, their propagation through a solid medium often creates multiple Lamb wave modes. The dispersive nature of waves means that the different frequency components of the Lamb waves travel at different speeds and that the shape of the wavepacket changes as it propagates through solid media. However, for damage detection applications, it may be useful to limit the number of generated Lamb waves to two fundamental modes, namely the S_0 and A_0 modes, and to select a less dispersive frequency region so that the interpretation of response signals becomes easier.

In this study, a Morlet wavelet with a narrowband driving frequency around 110 kHz is designed as the input waveform (see figure 2(a)). Several factors need to be taken into account for an appropriate selection of driving frequency. The first step in designing the input frequency is to compute the dispersion curve of the group velocities. While the application of effective elastic properties in composite laminates is limited, it is often useful to derive such constants for an initial estimate of the laminate response. Quasi-isotropic laminates exhibit in-plane isotropy in response to in-plane loading. For these laminates, the effective Young's modulus, Poisson's ratio and shear modulus may be defined which are the same for any direction within the plane of the laminate. These constants are obtained by rotating the stiffness tensor of each ply from the ply orientation angle to a common laminate direction. The transformed stiffnesses are then averaged over the thickness of the laminate, weighted by the thickness of each ply. The elements of the averaged stiffness tensor are related to effective elastic properties by analogy to an isotropic stiffness tensor [11]. Following this procedure, the effective Young's modulus and Poisson ratio of the composite plate are computed to be 5.5 GPa and 0.31, respectively. Then the velocities of P and S waves are computed from the following equations [2]:

$$V_P = \sqrt{(\lambda + 2\mu)/\rho}, \qquad V_S = \sqrt{\mu/\rho}, \tag{1}$$

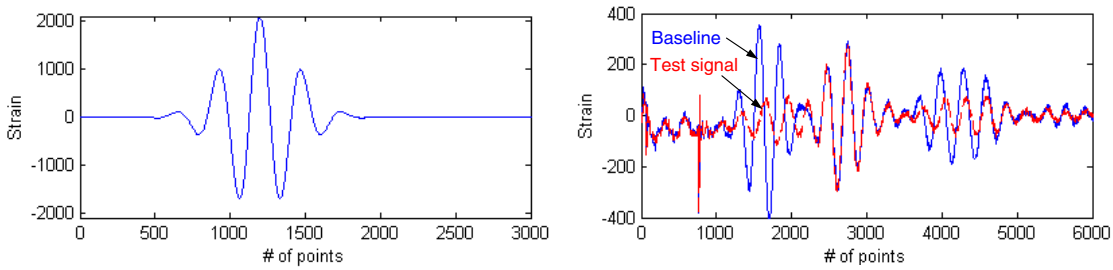

(a) An input Morlet waveform (b) Response strain time signals

Figure 2. Lamb wave time signals from the tested composite plate.

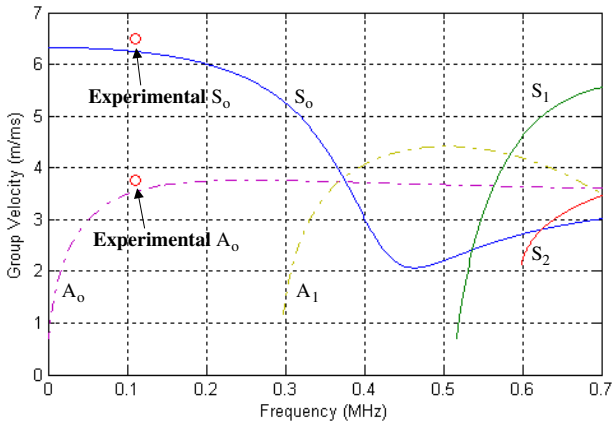

Figure 3. A dispersion curve for an idealized isotropic composite plate (the abscissa is presented in terms of the frequency with the given plate thickness (0.64 cm) rather than the frequency–thickness product).

where $\mu = E/2(1+\nu)$, $\lambda = \nu E/(1-2\nu)(1+\nu)$, E is the effective Young's modulus, ν is the Poisson ratio and ρ is the material density. Once the velocities of P and S waves are obtained, the dispersion curve shown in figure 3 is obtained by finding the Lamb wave solution for the wave equation [2, 12].

This dispersion curve is used to initially determine a frequency range where only the fundamental modes propagate and to find any non-dispersive regions. While the input frequency should be high enough to make the wavelength of the Lamb wave comparable to the scale of local damage, the driving frequency also needs to be low so that higher modes do not clutter the fundamental symmetric (S_0) and anti-symmetric (A_0) modes. A reasonable match between the experimental and analytical group velocities of the S_0 and A_0 modes are shown in figure 3. The experimental group velocities of the S_0 and A_0 modes are averaged values from several actuator–sensor paths and there are noticeable variations in the wave speeds, depending on the wave propagation directions along the composite plate. Note that the dispersion curve shown in figure 3 is computed for a macroscopically isotropic composite plate, although the plate tested in this study is anisotropic. Furthermore, the computation of the dispersion curve ignores damping effects in the composite plate. Therefore, the dispersion curve is used only as a guideline and several trial-and-error experiments are conducted to tune the optimal driving frequency value. For this experiment, the driving frequency is set to 110 kHz.

Figure 2(b) shows the time response of PZT patch no. 1 when the Morlet input waveform is generated at PZT patch no. 6. The numbering of the PZT patches is shown in figure 1(b). The full curve represents the baseline signal and the broken curve shows the response time signal when delamination is simulated within a direct line of the actuator and sensor path. The response signal is composed of several wave modes because of the dispersive nature of the excitation signal at the input frequency. From figure 2(b), it is observed that some modes are more sensitive to the simulated delamination than other modes. The first mode, which looks like a sine wave modulated by a cosine function in figure 2(b), is the first arrival of the A_0 mode associated with the direct path of wave propagation. The second mode is another A_0 mode that is reflected from the edge of the plate. (Note that the wave propagation path between PZT nos 1 and 6 pair is near the edge of the plate. See figure 1(b).) The observation of figure 2(b) clearly reveals that the first A_0 mode is the most sensitive to delamination damage. Although [5, 13] suggest that the S_0 mode is best for delamination detection, it was difficult to work with the S_0 mode in this particular example because the S_0 mode signal was too weak. This observation is similar to the findings in [5]. Therefore, only the A_0 mode was used in this study.

As a wave propagates through a solid medium, energy is transferred back and forth between kinetic and elastic potential energy. When this transfer is not perfect because of heating, wave leaking and reflection, attenuation occurs. In particular, the attenuation is increased by the presence of the delamination and the energy of the input force spills over from the driving frequency to neighboring frequency values. The energy loss in a damaged area is a result of the reflection and dispersion caused by micro-cracks within the laminate, resulting in the excitation of high frequency local modes. Based on these observations, a damage index is defined as the function of a signal's attenuation for a limited time span (a signal portion corresponding to the first A_0 mode) and at a specific frequency (the input frequency of the signal). Note that the attenuation is correlated to the amount of energy dissipated by the damage. In other words, the proposed damage index measures the degree of the test signal's energy dissipation compared to the baseline signal, especially at the first A_0 mode and at the input frequency value.

To achieve this goal, a wavelet transform is first utilized to obtain time–frequency information for the baseline signal [5]. This procedure is schematically shown in figures 4(a)–(c). In this study, the real Morlet wavelet is used for the family of

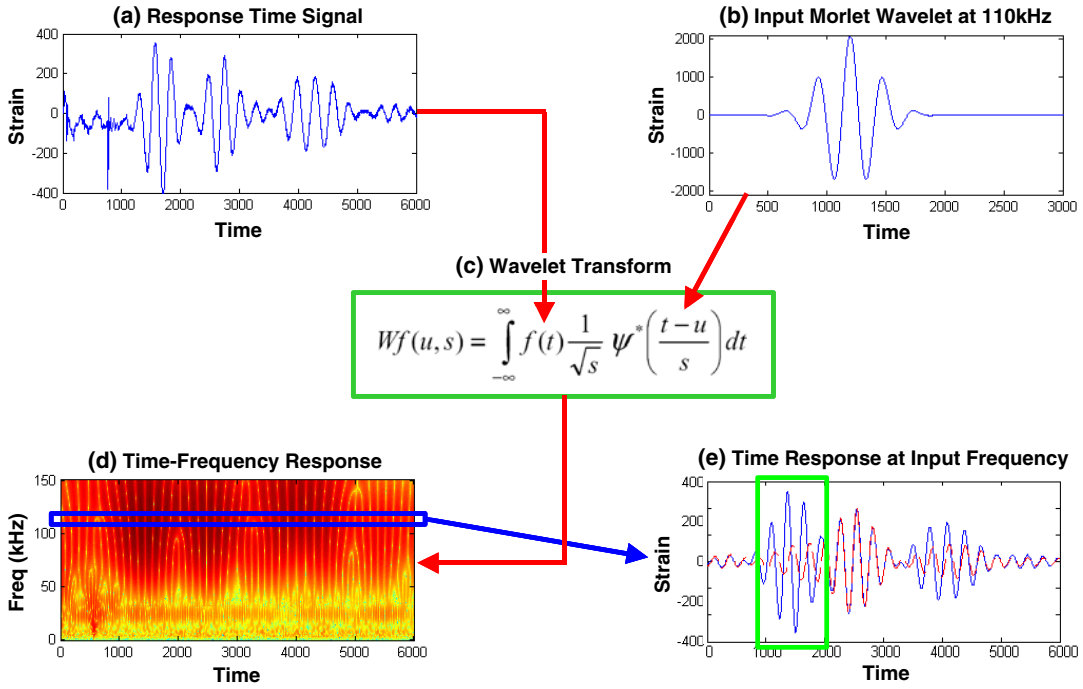

Figure 4. A wavelet analysis procedure to extract a damage-sensitive feature.

basis functions. (Note that the same Morlet wavelet is used as the input waveform in the experiment.) Because the shape of the actuating input is the same as the shape of the wavelet basis functions, the wavelet analysis procedure becomes more accurate and efficient [9, 14]. This wavelet, $\psi(t)$, is defined as

$$\psi(t) = \mathrm{e}^{-t^2/2}\cos(5t) \tag{2}$$

where 1500 data points are sampled between -4.2 and 4.2 of time t. Assuming the sampling rate of 20 MHz, this waveform results in a central frequency of 110 kHz. The wavelet transform, $Wf(u,s)$, is obtained by convolving the signal $f(t)$ with the translations (u) and dilations (s) of the mother wavelet:

$$Wf(u,s) = \int_{-\infty}^{\infty} f(t)\frac{1}{\sqrt{s}}\psi^*_{u,s}(t)\,\mathrm{d}t \tag{3}$$

where

$$\psi^*_{u,s}(t) = \frac{1}{\sqrt{s}}\psi\left(\frac{t-u}{s}\right). \tag{4}$$

Note that each value of the wavelet transform $Wf(u,s)$ is normalized by the factor $1/\sqrt{s}$ to ensure the integral energy given by each wavelet is independent of the dilation s.

Once the time–frequency information is obtained (figure 4(d)), the signal component corresponding only to the input frequency is retained for additional signal processing. By looking at this filtered view of the transmitted energy from the actuator to the sensor at the input frequency, one could gain an insight into how the intensities of the input energy have been shed into sideband frequencies as a result of damage. Then, the energy content of this baseline signal component is computed only at the first A_0 mode of the signal (figure 4(e)). These procedures (figures 4(a)–(e)) are then repeated for a test signal. Finally, the damage index (DI) is related to the ratio of the test signal's kinetic energy to that of the baseline signal:

$$\mathrm{DI} = 1 - \int_{u_0}^{u_1} Wf_{\mathrm{t}}(u,s_0)\,\mathrm{d}u \Big/ \int_{u_0}^{u_1} Wf_{\mathrm{b}}(u,s_0)\,\mathrm{d}u \tag{5}$$

where the subscripts b and t denote the baseline and test signals, u_0 and u_1 represent the starting and ending time points of the baseline signal's first A_0 mode and $0 \leqslant \mathrm{DI} \leqslant 1$. Note that the value of DI becomes zero when there is no attenuation of the test signal compared to the baseline signal and its value becomes larger as the test signal attenuates more as a result of damage.

4. Damage classification using extreme value statistics

Once the damage index value is computed, a method must be employed for determining a statistically rigorous threshold, whose exceedance indicates the presence of damage in a path. This establishment of the decision boundary (or the threshold) is critical to minimize false-positive and false-negative indications of damage. Although data are often assumed to have a normal distribution for building a statistical model for damage classification, it should be noted that a normal distribution weighs the central portion of data rather than the tails of the distribution. For damage detection applications, we are mainly concerned with extreme (minimum or maximum) values of the data because the threshold values will reside near the tails of the distribution. The solution to this problem is to use an approach called extreme value statistics (EVS) [15], which is designed to accurately model behavior in the tails of a distribution.

Suppose that one is given a vector of samples $\{X_1, X_2, \ldots, X_n\}$ from an arbitrary parent distribution. The

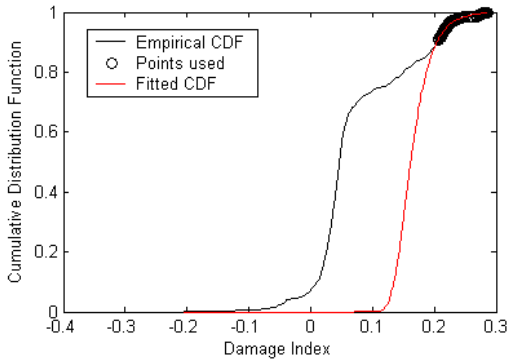

(a) Gumbel distribution curve-fitting
(Only top 10% of data is used for curve fitting)

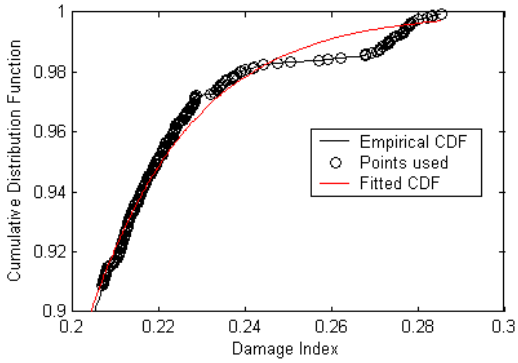

(b) Gumbel distribution curve-fitting
(Zoomed for top 10% of the damage index values)

Figure 5. Fitting of a Gumbel maximum distribution to the top 10% of damage index values.

most relevant statistic for studying the tails of the parent distribution is the maximum operator, $\max(\{X_1, X_2, \ldots, X_n\})$, which selects the point of maximum value from the sample vector. Note that this statistic is relevant for the right tail of a univariate distribution only. For the left tail, the minimum should be used. The pivotal theorem of EVS states that, in the limit as the number of vector samples tends to infinity, the induced distribution of the maxima can only take one of three forms: Gumbel, Weibull or Frechet [16]:

$$\text{FRECHET: } F(x) = \begin{cases} \exp\left[-\left(\dfrac{\delta}{x-\lambda}\right)^{\beta}\right] & \text{if } x \geqslant \lambda \\ 0 & \text{otherwise} \end{cases} \tag{6}$$

$$\text{WEIBULL: } F(x) = \begin{cases} 1 & \text{if } x \geqslant \lambda \\ \exp\left[-\left(\dfrac{\lambda-x}{\delta}\right)^{\beta}\right] & \text{otherwise} \end{cases} \tag{7}$$

$$\text{GUMBEL: } F(x) = \exp\left[-\exp\left(-\frac{x-\lambda}{\delta}\right)\right]$$
$$-\infty < x < \infty \quad \text{and} \quad \delta > 0. \tag{8}$$

In a similar fashion, there are only three types of distribution for the minima of the samples;

$$\text{FRECHET: } F(x) = \begin{cases} 1 - \exp\left[-\left(\dfrac{\delta}{\lambda-x}\right)^{\beta}\right] & \text{if } x \leqslant \lambda \\ 1 & \text{otherwise} \end{cases} \tag{9}$$

$$\text{WEIBULL: } F(x) = \begin{cases} 0 & x \leqslant \lambda \\ 1 - \exp\left[-\left(\dfrac{x-\lambda}{\delta}\right)^{\beta}\right] & x > \lambda \end{cases} \tag{10}$$

$$\text{GUMBEL: } F(x) = 1 - \exp\left[-\exp\left(\frac{x-\lambda}{\delta}\right)\right]$$
$$-\infty < x < \infty \quad \text{and} \quad \delta > 0 \tag{11}$$

where λ, α and β are the model parameters, which should be estimated from the data. Note that α and β should be greater than 0.

Now, given samples of maximum or minimum data from a number of n-point populations, it is possible to select an appropriate limit distribution and fit a parametric model to the data. It is also possible to fit a model to portions of the parent distribution's tails, as the distribution of the tails is equivalent to the appropriate extreme value distribution. Once the parametric model is obtained, it can be used to compute an effective threshold for damage detection based on the true statistics of the data, as opposed to statistics based on a blanket assumption of a Gaussian distribution. Details on parameter estimation of extreme value distributions can be found in [17].

In this study, the damage index value is computed from various normal conditions of the composite plate. Then, the statistical distribution of the damage index is characterized by using a Gumbel distribution, which is one of three types of extreme value distributions. λ and δ values in equation (8) are estimated to be 0.1536 and 0.0226, respectively. Figure 5 demonstrates how well the maximum values of the damage index can be fitted to a Gumbel distribution. Note that the Gumbel distribution is fitted only to the maximum 10% of the damage index values. From this fitted cumulative density function (CDF), a one-sided 99.9% confidence interval was determined, resulting in a threshold value of 0.29.

It should be noted that the computation of the threshold value based on EVS requires training data only from the undamaged conditions of a structure, classifying the proposed statistical approach as one of the unsupervised learning methods. Another class of statistical modeling is supervised learning where training data from both undamaged and damaged conditions are required. When a structural health monitoring system is deployed to real-world applications, it is often difficult to collect training data from various damage cases. Therefore, an unsupervised learning method, such as the one presented here, will be more practical in field applications. Furthermore, by properly modeling the maximum distribution of the damage index, false alarms have been minimized.

5. Experimental results

Because multiple damage cases needed to be investigated and there was only one composite plate available, delamination on the composite plate was simulated by attaching industrial putties in various locations. Because the putty attenuates the Lamb waves in a similar manner as delamination does, this material closely models the change of the Lamb wave

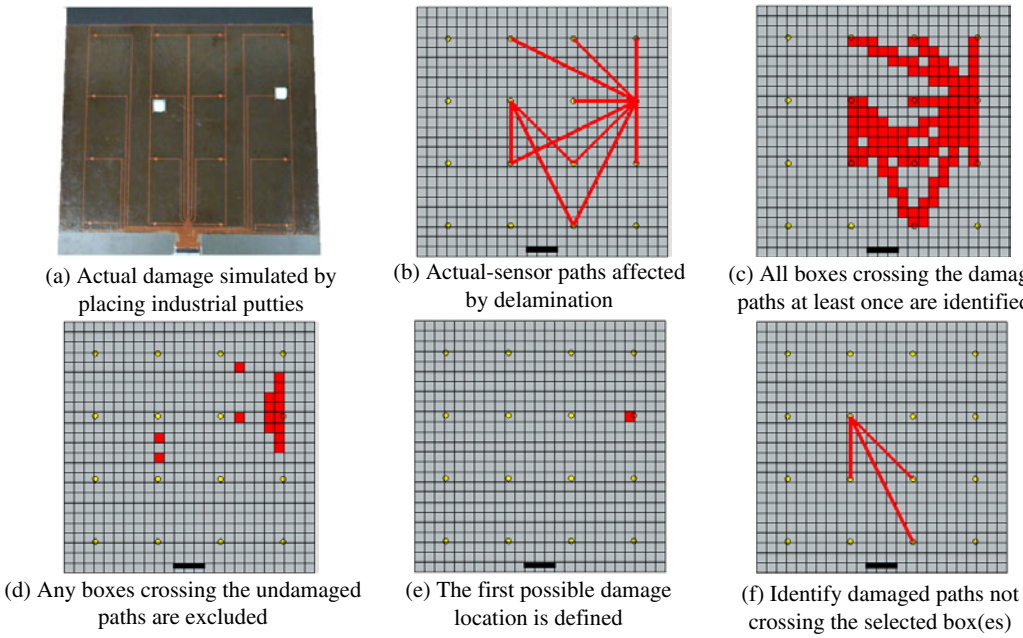

(a) Actual damage simulated by placing industrial putties
(b) Actual-sensor paths affected by delamination
(c) All boxes crossing the damage paths at least once are identified
(d) Any boxes crossing the undamaged paths are excluded
(e) The first possible damage location is defined
(f) Identify damaged paths not crossing the selected box(es)

Figure 6. Damage localization procedure using virtual grids.

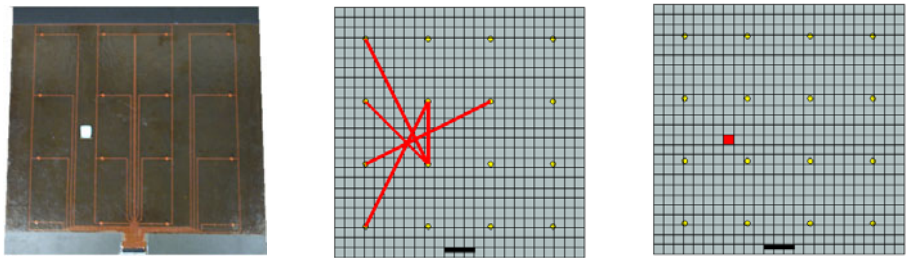

(a) Actual damage simulated by placing an industrial putty
(b) Actuator-sensor paths affected by the damage
(c) The damage identified by the proposed method

Figure 7. Detection of a single damage location using the wavelet-based approach.

characteristics that may be expected from delamination (see figure 6(a)). The size of the industrial putty patch was about 2.54 cm × 2.54 cm (1 in × 1 in).

First, the baseline signals corresponding to 66 different actuator and sensor paths were recorded at a known intact condition of the plate. Once delamination was simulated by placing the industrial putty at an arbitrary location on the composite plate, the test signals were recorded for the actuator and sensor combinations identical to the baseline case. Then, the damage index value defined in equation (5) was computed for each path. A given actuator–sensor path is classified as damaged when the value of the damage index becomes larger than 0.29. This threshold value for the damage index is established by using the previously described EVS. Figure 6(b) displays the actuator–sensor paths (damaged paths) affected by the simulated damage shown in figure 6(a). These damage paths have DI values greater than 0.29.

The next goal is to pinpoint the location of the delamination and to estimate its size based on the damaged paths identified in the previous step. To identify the location and area of the delamination, the composite plate is divided into 25-by-25 virtual grids, as shown in figure 6(b). The size of each grid is 2.44 cm × 2.44 cm (0.96 in × 0.96 in). The delamination shown in figure 6(a) is identified from the damaged paths previously detected in figure 6(b) based on the following rules:

(1) All boxes crossing the damaged paths at least once are identified (figure 6(c)).
(2) Any boxes crossing the undamaged paths, that have a damage index value less than or equal to 0.29, are excluded from possible damage locations (figure 6(d)).
(3) The box that has the largest number of the damaged paths crossing and zero undamaged paths crossing is selected as the first possible damage location (figure 6(e)).
(4) If there are any damaged paths left that are not crossing the damaged box(es) selected in the previous step, find a subset of the boxes that are crossing these remaining damaged paths and repeat steps (1)–(4) until there are no damaged paths left that are not crossing the selected boxes at least once (figure 6(f)).

Note that this last step (4) is necessary to detect multiple damage locations. In addition, a delamination area larger than one virtual grid size will be indicated by multiple boxes. The capability of the proposed method to detect single and multiple damage locations is successfully demonstrated in

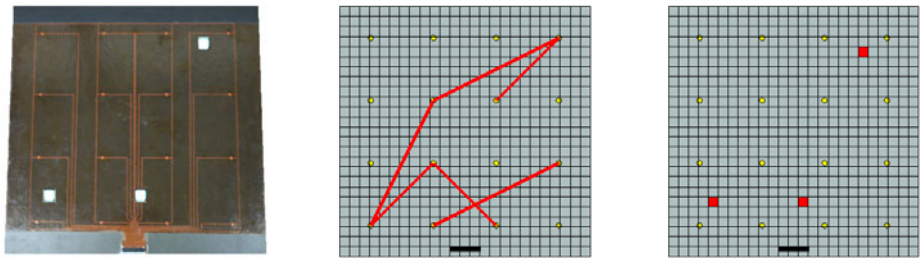

(a) Actual damage simulated by placing multiple industrial putties

(b) Actuator-sensor paths affected by the damage

(c) The damage identified by the proposed method

Figure 8. Detection of multiple damage locations using the wavelet-based approach.

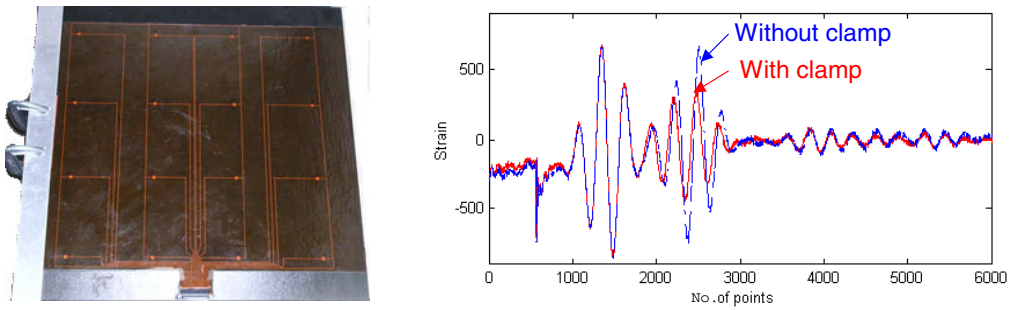

(a) One edge of the plate is clamped by an aluminum plate

(b) The response signals of the actuator (no.2) and sensor (no.3) pair

Figure 9. Change of the response signal as a result of a boundary condition change.

figures 7 and 8, respectively. Although it is not presented in this paper, different sizes of simulated delamination and industrial putties attached on the backside of the plate are also successfully detected. It is worthwhile noting that our damage localization method is solely based on the estimation of signal attenuation, unlike other methods that use the time-of-arrival information [5, 18]. Therefore, the proposed damage location approach can be easily applied to anisotropic composite plates because the wave speed variation in regards to the fiber orientation of the plate is irrelevant.

In real world applications, it is also important to demonstrate that structural health monitoring is robust when used under varying environmental and operational conditions. The effect of varying temperature and boundary conditions on the proposed damage detection algorithm is investigated. First, one edge of the plate is clamped using an aluminum plate, as shown in figure 9(a), and the associated response signal for the wave path of patches nos 2 and 3 is shown in figure 9(b). It is clearly demonstrated that the clamped boundary condition only changes the second A_0 wave of the signal reflected from the clamped edge of the plate (the second modulated sine wave in figure 9(b)). However, it does not affect the performance of the proposed damage detection algorithm at all because the damage index is based on the signal's attenuation only at the first A_0 mode.

Second, the influence of varying temperature on the damage detection algorithm is investigated. As shown in figure 10(a), one portion of the plate is heated using an industrial heat gun from 26 °C (78 °F) to 43 °C (110 °F) and 49 °C (120 °F), respectively. The responses corresponding to these three temperature conditions are shown in figure 10(b). The amplitude changes are negligible and only a small time delay of the response signals is observed. However, this time delay does not affect the performance of the damage index because the proposed damage detection again depends only on the signal's attenuation at the first A_0 mode. More extensive studies on the environmental and operational variations of the system are necessary to further demonstrate the robustness of the proposed damage detection system.

6. Summary and discussion

In this paper, a damage detection algorithm is developed to identify the location and area of delamination on a quasi-isotropic graphite/epoxy composite plate. A unique input waveform to drive PZT actuators and a signal processing analysis technique are developed based on wavelet analysis. In addition, a statistically rigorous damage classifier is incorporated based on extreme value statistics to minimize false indications of damage. By using the proposed input waveform and signal processing technique, the proposed damage detection algorithm was able to properly detect simulated delamination on a composite plate even in the presence of varying temperature and boundary conditions. Finally, the approach presented herein is very attractive for the development of an automated continuous monitoring system because of its simplicity and minimal interaction with users.

However, it should be pointed out that the procedure developed has only been verified on relatively simple laboratory test specimens. To fully verify that the proposed approach is truly robust, it will be necessary to test the proposed approach for a wide range of operational and environmental cases and for different representative damage types, such as ply crack, fiber breakage and through-hole penetrations. In

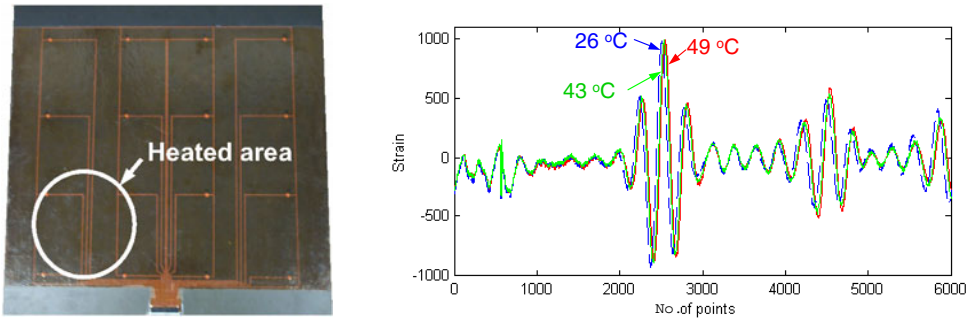

(a) Temperature of one corner of the plate is increased from 26 °C to 43 °C and 49 °C

(b) The response signals of the actuator (no.1) and sensor (no.6) pair

Figure 10. Change of the response signal as a result of temperature variation.

addition, the minimum size of detectable delamination depends on the spacing of the PZT patches, selection of the actuating frequency, the size of the virtual grids and the wavelength of the transmitted waves. In general, users will specify the minimum size of delamination that they want to detect. Then, the aforementioned design parameters need to be optimized to ensure that the specified minimum delamination can be detected. Further research is warranted to optimize these design parameters. A follow-up experiment is underway to seed initial delamination into composite structures by impact testing and to grow the delaminated area by cyclic load testing. The proposed system will be continuously used to monitor the growth of delamination during these tests.

Acknowledgments

Funding for this project was provided by the Department of Energy through the internal funding program at Los Alamos National Laboratory known as Laboratory Directed Research and Development (Damage Prognosis Solutions). The authors acknowledge Acellent Technologies, Inc. for providing technical support for their hardware system.

References

[1] Bourasseau N, Moulin E, Delebarre C and Bonniau P 2000 Radome health monitoring with lamb waves: experimental approach *NDT&E Int.* **33** 393–400

[2] Kessler S S 2002 Piezoelectric-based *in situ* damage detection of composite materials for structural health monitoring systems *PhD Dissertation* MIT, MA

[3] Staszewski W J, Pierce S G, Worden K and Culshaw B 1999 Cross-wavelet analysis for Lamb wave damage detection in composite materials using optical fibre *Key Eng. Mater.* **167/168** 373–80

[4] Badcock R A and Birt E A 2000 The use of 0-3 piezocomposite embedded Lamb wave sensors for detection of damage in advanced fibre composites *Smart Mater. Struct.* **9** 291–7

[5] Lemistre M and Balageas D 2001 Structural health monitoring system based on diffracted Lamb wave analysis by multiresolution processing *Smart Mater. Struct.* **10** 504–11

[6] Okafor A C, Chandrashekhara K, Jiang Y P and Kilcher R R 1994 Damage assessment of smart composite plates using piezoceramic and acoustic emission sensors *Proc. SPIE* **2191** 265–75

[7] Monnier T, Guy P, Jayet Y, Baboux J C and Salvia M 2000 Health monitoring of smart composite structures using ultrasonic guided waves *Proc. SPIE* **4073** 173–81

[8] Acellent Technologies, Inc. 2003 http://www.acellent.com/

[9] Abbate A, Koay J, Frankel J, Schroeder S C and Das P 1997 Signal detection and noise suppression using a wavelet transform signal processor: application to ultrasonic flaw detection *IEEE Trans. Ultrason. Ferroelectr. Freq. Control* **44** 14–26

[10] Lamb H 1917 On waves in an elastic plate *Proc. R. Soc.* A **93** 293–312

[11] Gürdal Z, Haftka R T and Hajela P 1998 *Design and Optimization of Laminated Composite Materials* (New York: Wiley)

[12] Vallen System: The Acoustic Emission Company 2003 http://www.vallen.de/

[13] Tan K S, Guo N, Wong B S and Tui C G 1995 Experimental evaluation of delaminations in composite plates by the use of lamb waves *Compos. Sci. Technol.* **53** 77–84

[14] Lind R, Kyle S and Brenner M 2001 Wavelet analysis to characterize non-linearities and predict limit cycles of an aeroelastic system *Mech. Syst. Signal Proc.* **15** 337–56

[15] Sohn H, Allen D W, Worden K and Farrar C R 2003 Structural damage classification using extreme value statistics *ASME J. Dyn. Syst. Meas. Control* at press

[16] Fisher R A and Tippett L H C 1928 Limiting forms of the frequency distributions of the largest or smallest members of a sample *Proc. Camb. Phil. Soc.* **24** 180–90

[17] Castillo E 1998 *Extreme Value Theory in Engineering* (*Academic Press Series in Statistical Modeling and Decision Science*) (San Diego, CA: Academic)

[18] Wang C S and Chang F K 2000 Diagnosis of impact damage in composite structures with built-in piezoelectrics network *Proc. SPIE* **3990** 13–9